

Adsorptive removal of crystal violet using agricultural waste: Equilibrium, kinetic and thermodynamic studies

Nnaemeka J. Okorochoa¹, Conrad K. Enenebeaku², Maureen O. Chijioke-Okere³, Chinyere E. Ohaegbulam⁴, Cynthia E. Ogukwe⁵

¹(Department of pure and industrial chemistry, College of physical sciences/ University of Calabar, Nigeria)

^{2,3,4,5}(Department of chemistry, college of physical sciences/ Federal University of Technology Owerri, Nigeria)

Corresponding Author: Nnaemeka J. Okorochoa

ABSTRACT: The potential of raw cassava peels powder, RCP for the removal of crystal violet (CV) dye from aqueous solution was investigated. The adsorbent was characterized by Fourier transform infra-red spectrophotometer, FTIR and Scanning electron microscope, SEM analysis. Batch adsorption studies were conducted and various parameters such as contact time, adsorbent dosage, initial dye concentration, pH and temperature were studied to observe their effects in the dye adsorption process. The optimum conditions for the adsorption of CV onto the adsorbent (RCP) was found to be: contact time (60mins), pH (10.0) and temperature (303K) for an initial CV dye concentration of 100mg/l and adsorbent dose 1.0g. The experimental equilibrium adsorption data fitted best and well to the Dubinin-Radushkevich (D-R) isotherm model. The maximum adsorption capacity was found to be 26.63mg/g. The kinetic data conformed to the pseudo-second-order kinetic model, suggesting that the rate limiting step may be chemisorptions. Adsorption mechanism indicated that intra-particle diffusion was not the rate limiting step. Thermodynamic quantities evaluated revealed negative values of ΔG^0 , ΔH^0 and ΔS^0 obtained indicating the spontaneous and exothermic nature of the adsorption process.

Keywords: Adsorption, Cassava peels powder, Crystal violet, Isotherms, Kinetics

Date of Submission: 28-08-2019

Date of acceptance: 13-09-2019

I. INTRODUCTION

Dyes are natural or synthetic colored organic compounds having the property of imparting their color to other substances or substrates to which it is being applied. Most dyes are aromatic, reactive, non biodegradable and of synthetic origin. Synthetic dyes have added advantages over natural dyes in terms of permanence, quick setting, easy to use, color range, availability and are ensured by accurate formulas [1]. There are more than 10,000 commercially available dyes with over 7×10^5 tones of dyestuff being produced annually across the world today [2]. Dyes are widely used in various industries such as food, paper, rubber, cosmetics, plastics, tannery, paint, pharmaceuticals, carpet and textile to color their products which generate a large volume of colored waste water annually [3, 4]. It is estimated that 2% of dyes produced annually are discharged in effluents from these associated industries [5]. The disposals of these dye based effluents have been an increasing worldwide concern for the last few decades.

Crystal Violet (CV) is an N-methylated triaminotriphenylmethane dye most widely used for coloring purpose among all other dyes of its category [6]. This basic (cationic) dye is generally used for the dyeing of cotton, wool, silk, leather, nylon, paper etc. In fact basic dyes, such as crystal violet, are the brightest class of soluble dyes whose tinctorial values are very high; less than 1 mg/L of the dye produces an obvious coloration. The coloration of water by these dyes may have an inhibitory effect on photosynthesis as a result of lack of light penetration, thus affecting aquatic ecosystems [7, 8]. Some of the dyes or their metabolites are either toxic or mutagenic and carcinogenic [9]. It is therefore necessary to remove these dyes from effluents (or wastewater) with a suitable technology before discharging it into receiving water bodies.

Over the past few decades, several processes or methods have been used for the removal of dyes from wastewater such as biological (aerobic and anaerobic), chemical precipitation, coagulation/ flocculation, solvent extraction, membrane filtration, ion exchange, ozonation, electrochemical destruction and adsorption [10,11]. Adsorption process has simplicity of design, more efficient, easy to operate, insensitivity to toxic substances and

cost effective, hence, it has been suggested as a potential alternative to the existing physical / chemical /biological methods for the removal of dyes from industrial effluents or waste water [1]. A number of investigations carried out using agricultural materials or the wastes and by product of industries for the removal of dyes from aqueous solutions have been reviewed [12]. However, research interest into production of more new economical, easily available and highly efficient adsorbents are still under development. Hence attempts are made in this study to develop a low-cost adsorbent for wastewater treatment using cassava peels powder.

Cassava (*Manihot esculenta*) belonging to the family Euphorbiaceae is extensively cultivated as an annual crop for its edible starchy tuberous root, a major source of carbohydrates in Nigeria and West Africa region. Nigeria is the world's largest producer of cassava, and its peels are left in the fields after harvest and during processing. Therefore, the availability of cassava peels is vast in Nigeria. The objectives of this study were to investigate and examine the possibility of using cassava peels powder for adsorption of Crystal Violet (CV) from aqueous solutions in batch system. The effects of adsorbent dosage, contact time, initial dye concentration, pH and temperature on CV dye adsorption using cassava peels powder were investigated. Adsorption isotherms, kinetics, mechanism and thermodynamic parameters were also evaluated and reported.

II. MATERIALS AND METHOD

2.1 Adsorbent Collection and Preparation

The raw cassava peels were collected from cassava fields of FUTO, Owerri, Nigeria. This agricultural waste was washed thoroughly with water to remove sand, dirt and other impurities present in it and sundried until all moistures were removed. It was then ground in a mill and sieved in a sieve shaker of particle size 80 μ m. The raw cassava peels powder that passed through the sieve were stored in an air tight container and used as adsorbent without any further pretreatment.

2.2 Preparation of Adsorbate Solutions

Analytical grade CV dye (C.I.N: 42555, molecular formula: $C_{25}H_{30}N_3Cl$, molecular weight: 407.98, $\lambda_{max} = 590$ nm) was obtained from a laboratory. A stock solution of CV dye of concentration 1000 mg/L was prepared by dissolving 1g of powder CV dye in 1L of distilled water. Experimental dye solutions of desired concentration were obtained by appropriate dilution of the stock solution.

2.3 Adsorbent Characterization

Fourier transform infra-red (FTIR) spectrophotometer was used to identify the different functional groups available on the adsorbent sites and their effect on dye adsorption. The FTIR of the adsorbent was taken before adsorption using FTIR spectrophotometer (Shimadzu-8400S). 0.1g of the adsorbent was encapsulated with 1g of KBr spectroscopy grade (merk, Darmstadt, Germany) and by introducing the mix in a piston's cell of a hydraulic pump with compression pressure 15KPa/cm² the solid translucent disk was obtained which was introduced in an oven for 4hrs at 105⁰C to ensure the non interference of any existing water vapour or CO₂ molecules. The FTIR spectrum was then recorded within the wave number range 4000 – 450. In addition, surface morphology and texture of the adsorbent was analyzed using scanning electron microscope (SEM) (Model-PHENOM ProX). Prior to scanning, some quantity of the adsorbent was placed on a double adhesive sticker placed in a sputter machine for 5 sec; this gave the adsorbent a conductive property. Sample (adsorbent) stud was fixed on a charge reduction sample holder, and then was charged in the SEM machine.

2.4 Batch Adsorption Experiments

Batch adsorption of CV dye onto the adsorbent (RCP) was conducted in a 250ml airtight Erlenmeyer flask containing 100ml of known concentration of the CV dye solution and an accurately weighed amount of the adsorbent. The mixtures in the flasks were agitated on a mechanical shaker operating at a constant speed of 150 rpm. The effect of contact time (15, 30, 45, 60, 90 & 120 min), adsorbent dosage (0.5, 1, 1.5, 2 & 3 g/L), initial CV dye concentration (40, 80, 100, 120 & 140 mg/l), pH (2, 4, 6, 8, 10 & 12) and temperature (303, 313, 323, 333 & 343 K) were evaluated. The flask containing the samples were withdrawn from the shaker at predetermined time intervals, filtered and the final concentrations of CV dye in the supernatant solutions were analyzed using the UV-visible spectrophotometer (Model Hitachi – 2800). The pH of the solution was adjusted using 1M HCl or NaOH. The amount of equilibrium uptake of CV dye was determined using:

$$q_e = \frac{(C_o - C_e)V}{M} \quad (1)$$

$$\% \text{ Dye Removal} = \frac{(C_o - C_e)V}{C_o} \times 100 \quad (2)$$

Where q_e is the amount of dye taken up by the adsorbent at equilibrium (mg/g), C_o is the initial dye concentration (mg/L), C_e is the dye concentration at equilibrium (mg/L), M is the mass of the adsorbent (g), and V is the volume of the solution, (L)

III. THEORY

Different adsorption isotherm models have been used to describe the sorption equilibrium. Langmuir, Freundlich, Harkins and Jura, Dubinin–Raduskevich (D–R), Halsey, and Temkin isotherm models were applied in the present study.

3.1 Adsorption Isotherm

3.1.1 Langmuir Isotherm

The Langmuir model describes the monolayer adsorption. It assumes a uniform energy of adsorption, a single (homogenous) layer of adsorbed solute at a constant temperature [12, 13]. The linear form of langmuir equation is given as:

$$\frac{C_e}{q_e} = \frac{1}{q_m K_L} + \frac{C_e}{q_m} \quad (3)$$

Where q_e (mg/g) is the amount of dye adsorbed at equilibrium, q_m (mg/g), the amount of dye adsorbed when saturation is attained, C_e is the equilibrium dye concentration (mg/L) and K_L is Langmuir constant related to the binding strength of dye onto the adsorbent.

3.1.2. Freundlich Isotherm

The basic assumption of this model is that there is an exponential variation in site energies of adsorbent and also the fall in heat of adsorption is logarithmic [14]. The linearized form of Freundlich equation is expressed as:

$$\log q_e = \log K_f + \frac{1}{n} \log C_e \quad (4)$$

Where K_f and n are the Freundlich constants that represent adsorption capacity and intensity (or strength) of adsorption respectively. The significance of n is as follows: $n = 1$ (linear); $n < 1$ (chemical process); $n > 1$ (physical process) [15].

3.1.3. Harkins and Jura Isotherm

The Harkins and Jura adsorption isotherm model accounts for multilayer adsorption and can be explained by the existence of a heterogeneous pore distribution (12). The Harkins and Jura equation can be expressed as:

$$\frac{1}{q_e^2} = \frac{B}{A} - \frac{\log C_e}{A} \quad (5)$$

Where B and A are the isotherm constants and can be obtained from the intercept and slope of the plot of $1/q_e^2$ versus $\log C_e$ respectively.

3.1.4. Halsey Isotherm

The Halsey adsorption isotherm model is suitable for multilayer adsorption at a relatively large distance from the surface and the fitting of the experimental data to this equation attest to the heteroporous nature of the adsorbent [16, 17]. The Halsey adsorption isotherm model can be expressed as:

$$\ln q_e = \frac{\ln k}{n_H} - \frac{\ln \left(\frac{1}{C_e}\right)}{n_H} \quad (6)$$

Where n_H and K are Halsey isotherm constants and can be obtained from the slope and intercept of the plot of $\ln q_e$ against $\ln (1/C_e)$.

3.1.5. Temkin Isotherm

Temkin isotherm model assumes that the fall in the heat of adsorption is linear rather logarithmic as stated in Freundlich expression [12]. The heat of adsorption of all molecules in the layer would decrease linearly

with coverage owing to the adsorbent/adsorbate interactions [18-20]. The linearized form of Temkin equation is expressed as:

$$q_s = B \ln K_T + B \ln C_s \quad (7)$$

Where K_T (mol/L) is the equilibrium binding constant corresponding to maximum binding energy, B is the constant related to the heat of adsorption and the differential surface capacity for the dye sorption per unit binding energy. If the constant B is less than 8kJ/mol, it indicates a weak interaction between the adsorbate and adsorbent hence such adsorption can be expressed as physical adsorption [15, 21].

3.1.6. Dubinin-Radushkevich (D-R) Isotherm

The Dubinin-Radushkevich (D-R) isotherm model can be expressed as [15]:

$$\ln q_s = \ln q_s - \beta \varepsilon^2 \quad (8)$$

Where β is a constant related to the mean free energy of adsorption per mol of the dye ($\text{mol}^2 \text{kJ}^{-2}$) when it is transferred to the surface of the adsorbent from infinity in solution, q_s is the theoretical saturation capacity, ε is the Polanyi potential given as:

$$\varepsilon = RT \ln \left(1 + \frac{1}{C_s} \right) \quad (9)$$

Where R ($\text{J} \cdot \text{mol}^{-1} \cdot \text{K}^{-1}$) is a gas constant, T (K) is temperature. By making certain assumptions, the mean energy of adsorption E , can be calculated from the β value employing, the relation:

$$\frac{E}{\sqrt{2\beta}} = \quad (10)$$

3.2. Adsorption Kinetics

The pseudo-first-order, pseudo-second-order, power function, Elovich and intraparticle diffusion kinetic models were applied to study the adsorption kinetics of CV and to compute the extent of uptake in the adsorption process.

3.2.1. Pseudo-First-Order Kinetic Model

The linear form of the pseudo-first-order kinetic mode is represented by:

$$\ln(q_e - q_t) = \ln q_e - K_1 t \quad (11)$$

where q_e and q_t are the values of amount of the dye adsorbed per unit mass on the adsorbent at equilibrium and at various time t , respectively, K_1 is the Pseudo-first-order adsorption rate constant (min^{-1}). The values of K_1 and calculated q_e can be determined from the slope and intercept respectively, of the linear plot of $\ln(q_e - q_t)$ versus t .

3.2.2. Pseudo-Second-Order Kinetic Model

The pseudo-second-order kinetic model is expressed by:

$$\frac{t}{q_t} = \frac{1}{k_2 q_s^2} + \frac{1}{q_s} t \quad (12)$$

Where K_2 is the pseudo-second-order adsorption rate constant ($\text{g/mg} \cdot \text{min}$) and q_e is the amount of dye adsorbed (mg/g) on the adsorbent at equilibrium. The initial adsorption rate, h ($\text{mg} \cdot \text{g}^{-1} \cdot \text{min}^{-1}$) is expressed as:

$$h = k_2 q_s^2 \quad (13)$$

The plot of t/q_t versus t gives a linear relationship which allow computation of k_2 , h and calculated q_e . Among these models, the criterion for their applicability is based on judgment on the respective correlation coefficient (R^2) and agreement between experimental and calculated value of q_e [15, 22, 23].

3.2.3. Intra-particle Diffusion Model

The intra-particle diffusion model is expressed by [12, 22]:

$$Q_t = K_i t^{1/2} + C \quad (14)$$

Where C is the intercept which represents the effect of boundary layer thickness and K_i is the intra particle diffusion rate constant ($\text{mg} \cdot \text{g}^{-1} \cdot \text{min}^{1/2}$), which can be evaluated from the slope of a linear plot of q_t versus $t^{1/2}$.

If the plot of q_t versus $t^{1/2}$ gives a straight line, then the intra particle diffusion is involve in the adsorption process also if this line passes through the origin then the intra particle diffusion is the sole rate controlling step in the adsorption process. However, if the plot of q_t versus $t^{1/2}$ appears as multi linear plots, then two or more steps influence the adsorption process such as film diffusion and intra particle diffusion [15, 22, 24, 25].

3.3. Thermodynamic parameters

The thermodynamic parameters such as change in Gibb's free energy change (ΔG^0), enthalpy (ΔH^0) and entropy (ΔS^0) were determined using the following equations:

The Gibb's free energy, ΔG , equation is expressed as follows [26, 27]:

$$\Delta G = -RT \ln K_{ads} \quad (15)$$

The equilibrium constants (K_{ads}) were calculated according to the following equation:

$$K_{ads} = \frac{(q_e^m)}{(C_e)} \quad (16)$$

Where: R is gas constant ($8.314 \text{ J mol}^{-1} \text{ K}^{-1}$) and T is absolute temperature in Kelvin, q_e^m is dye concentration on

the solid at equilibrium and C_e is dye concentration in solution at equilibrium.

The Van't Hoff equation is expressed as follows [26, 27]:

$$\ln K_{ads} = \frac{\Delta S^0}{R} - \frac{\Delta H^0}{RT} \quad (17)$$

Where R is gas constant, T is absolute temperature in Kelvin, ΔS^0 and ΔH^0 are entropy and enthalpy respectively. The plot of $\ln K_{ads}$ versus $1/T$ gives a linear relationship, which allows the computation of ΔH^0 and ΔS^0 values from the slope and intercept respectively.

IV. RESULTS AND DISCUSSION

4.1. Characterization of the RCP Adsorbent

The FTIR spectral of RCP were obtained using KBr pellets within the spectral range of $4000\text{-}400 \text{ cm}^{-1}$ and is shown in Fig. 1. It can be observed that broad and minor peaks are present in the spectra such as peaks at 3872.23 cm^{-1} due to hydroxyl group, OH, attributed to adsorbed water, broad peak at 3453.34 cm^{-1} due to O-H bond from carboxylic acid, 2388.92 cm^{-1} due to N-H bond, 2267.48 cm^{-1} due to $\text{C}\equiv\text{C}$ bond, or $\text{C}\equiv\text{N}$, 1647.26 cm^{-1} due to $\text{C}=\text{C}$ bond from alkene, 1437.98 cm^{-1} due to symmetrical aliphatic bonding of methyl group, CH_3 , 1187.23 cm^{-1} due to C-N bond 1034.84 cm^{-1} due to C-O bond confirming presence of carboxylic acid, 641.35 cm^{-1} due to C-Cl bond, [22, 28].

Furthermore, Fig. 2 shows the SEM images of RCP. It can be observed from Fig. 2a that the external surface of RCP is uneven and irregular. On further magnification as indicated in 2b, the surface is very rough and contains heterogenous pores.

FTIR- 8400S FOURIER TRANSFORM INFRARED SPECTROPHOTOMETER

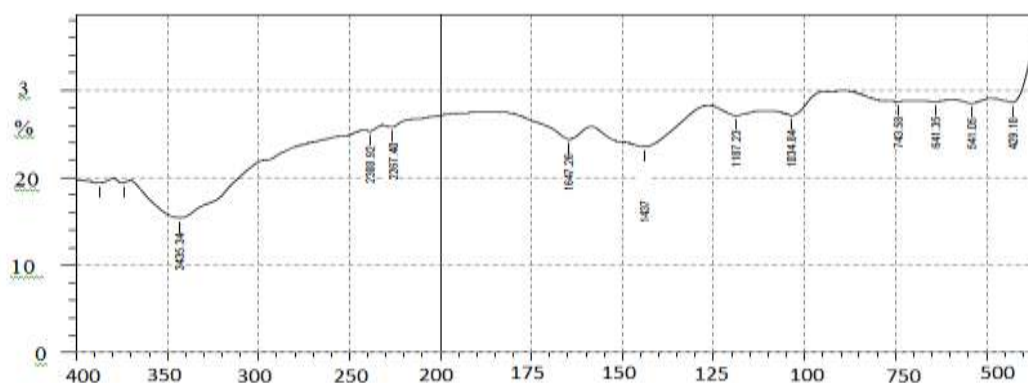


Fig. 1: FTIR spectra of RCP powder

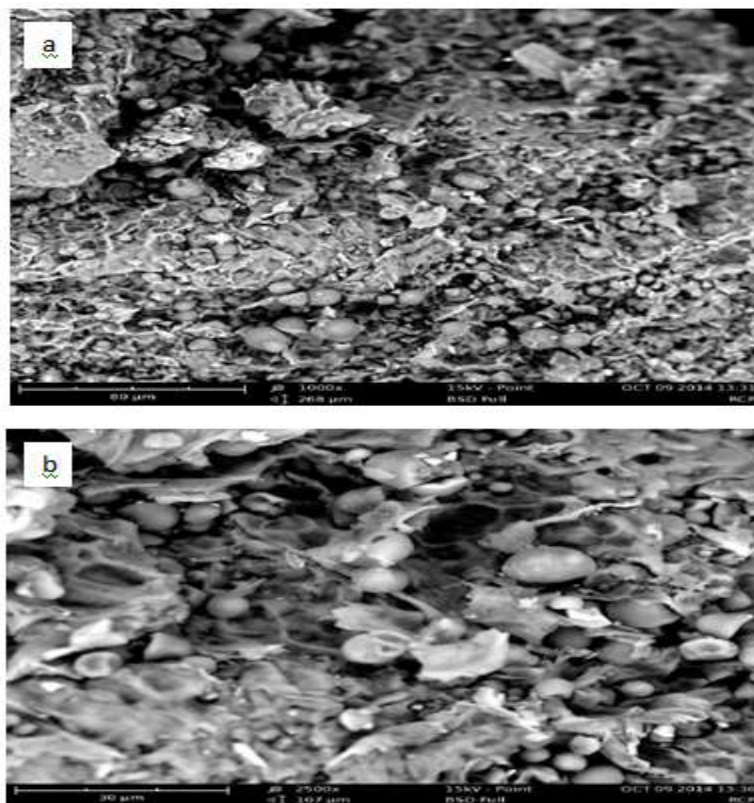


Fig.2 SEM images of RCP powder surface (a) magnification 1000× and (b) magnification 2500×

4.2. Effect of Contact Time

Contact time is an important parameter in the adsorption process. The effect of contact time on the removal of CV dye is depicted in Fig. 3. It can be observed that there was a rapid removal in the first 15 minutes and it proceeds slowly until optimum adsorption (equilibrium time) at 60 minutes. Later it decreases. Similar result was reported by Jyoti and Shakti [29]. It can be inferred from the rapid sorption rate at the initial stages that there were abundance of active sites on the external surface of RCP which resulted in the rapid CV dye removal. The slower rate of removal at the later stages can be attributed to the diffusion of the dyes into the interior part of the adsorbent since the external surface has been occupied by the molecules of the dye [30]. Once equilibrium is attained, the removal efficiency decreased due to the fact that the remaining vacant sites are difficult to occupy probably caused by repulsive forces between the molecules on the adsorbents and the bulk phase [31, 32].

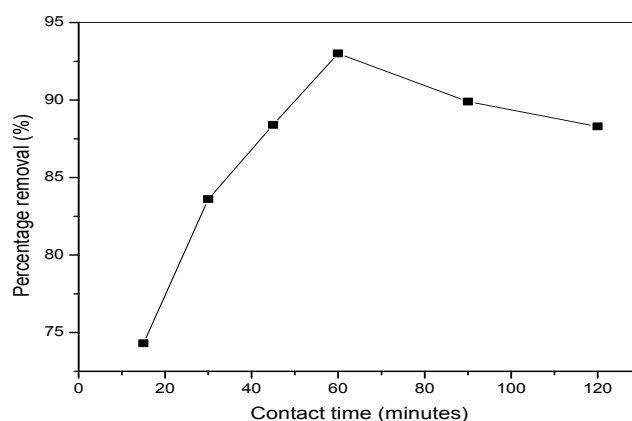


Fig. 3: Effect of contact time on percentage removal of CV dye (CV concentration: 100mg/l, adsorbent dosage: 1.0g, volume of solution: 100ml temperature: 300±1 K)

4.3. Effect of Adsorbent Dosage

The effect of adsorbent dosage on the percentage removal (or removal efficiency) of CV dye is depicted in Fig.4. It can be observed that the removal efficiency of CV dye increased with increase in adsorbent dosage. This observation can be attributed to the fact that the number of active sites on RCP surface increased with the increase in the adsorbent (RCP) dosage [15]. Although the percentage removal of CV dye increased with increase of adsorbent dosage, the equilibrium adsorption capacity decreased with increase of adsorbent dosage. This may be due to overlapping or aggregation of the active or adsorption sites which limits the availability of all the active sites during adsorption process [8, 33]. Similar trend has been reported for the adsorption of CV dye by different natural materials [8].

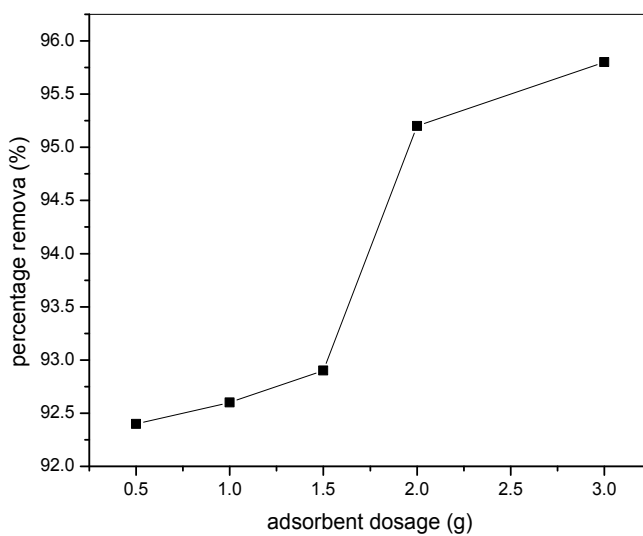


Fig.4: Effect of adsorbent dosage on percentage removal of CV dye (CV concentration: 100mg/l, contact time: 60mins, volume of solution: 100ml and temperature $300\pm 1K$)

4.4. Effect of Initial Dye Concentration

The effect of initial CV dye concentration is depicted in Fig. 5. It can be observed that the removal efficiency of CV dye increased with increase in initial concentration. This observation may be due to the fact that with increase in dye concentration, more dye molecules are available for adsorption by the adsorbent. This is attributed to the effect of concentration gradient which is the main driving force for the adsorption process [34]. Similar trend has been reported by Asiagwu et al. [35]. Furthermore, the equilibrium adsorption capacity increased with increase in initial dye concentration (figure not shown). This is attributed to the fact that increasing CV dye concentration increases the driving force to overcome all mass transfer resistance of CV between the aqueous and solid phase, leading to an increasing equilibrium adsorption capacity [15, 36].

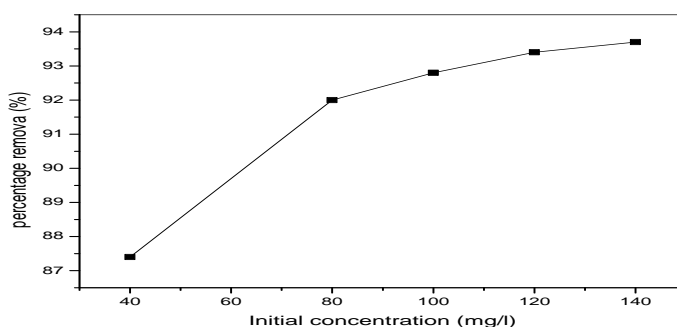


Fig. 5: Effect of initial concentration on percentage removal of CV dye (Contact time: 60mins, Adsorbent dosage: 1g, volume of solution: 100ml and temperature $300\pm 1K$).

4.5. Effect of pH

The pH of the dye solution is an important parameter in the adsorption process and the initial pH of dye solution has greater significance compared to the final pH of the solution in adsorption reaction [37]. The influence of pH on the adsorption of CV onto RCP is illustrated in Fig. 6. It was observed that the removal efficiency of CV by RCP increased as the initial pH of the solution increased from 2 to 12. Similar trend have been observed for the adsorption of CV by different natural materials [8]. Optimum removal efficiency was obtained at pH of 10.0. The decrease in removal efficiency at low pH can be attributed to the fact that at low pH values of the solution, the presence of excess hydrogen ion in the solution competes with the cationic groups of the CV dye for the adsorption sites on the adsorbent surface [38]. However, at higher pH values, the positive charges (H^+) at the solution interphase or adsorption sites decreases and the adsorbent surface is more negatively charged, thus enhancing electrostatic attraction of the cations of the CV dye leading to more removal efficiency.

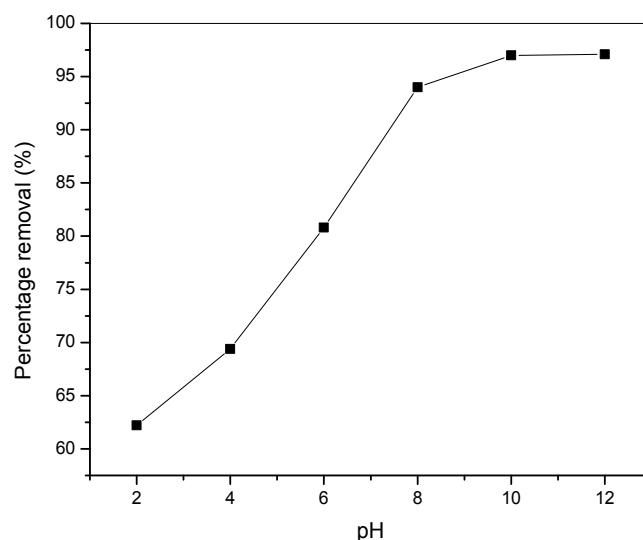


Fig.6: Effect of pH on percentage removal of CV dye (contact time: 60mins, CV concentration: 100mg/l, adsorbent dosage: 1g, volume of solution: 100ml and temperature $300\pm 1K$).

4.6. Effect of Temperature

The influence of temperature on the removal efficiency of CV by RCP is illustrated in Fig. 7. It can be observed that increase in temperature resulted in decrease in removal efficiency of CV by RCP. This observation suggests that the adsorption of CV dye by raw cassava peels powder is an exothermic process. Similar observation has been reported for the adsorption of CV dye by date palm fiber [26]. This decrease in removal efficiency with increase in temperature can be attributed to the weakening of the physical bonding between the adsorbate (CV dye molecules) and the active sites of the adsorbent (RCP). The CV dye solubility also increased with increase in temperature resulting in the interaction between the solute and the solvent to be stronger than that between the solute and the adsorbent. Consequently the solute was more difficult to adsorb [39, 40].

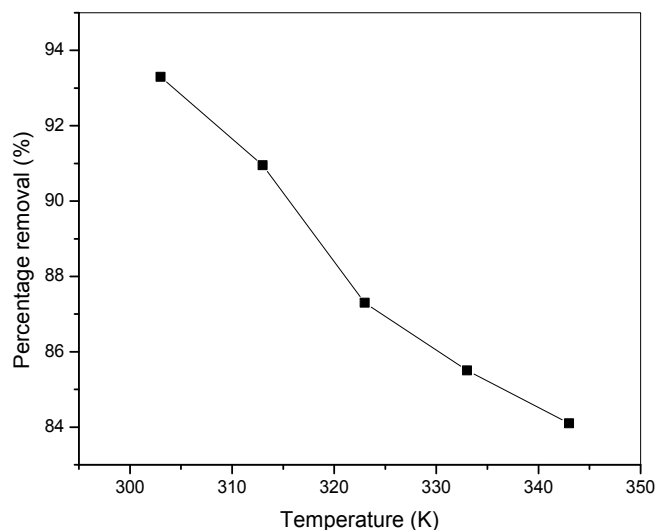


Fig.7: Effect of temperature (CV concentration: 100m/l, adsorbent dose: 1g, volume of solution: 100 ml and contact time: 60 mins)

4.7. Adsorption Isotherms

Six adsorption isotherm models were applied to describe the relationship between the CV dye concentration in the bulk solution and that on the RCP powder's surface namely, the Langmuir, Freundlich, Harkins and Jura, Dubinin–Raduskevich (D–R), Halsey, and Temkin isotherm models. The results are shown in Table 1.

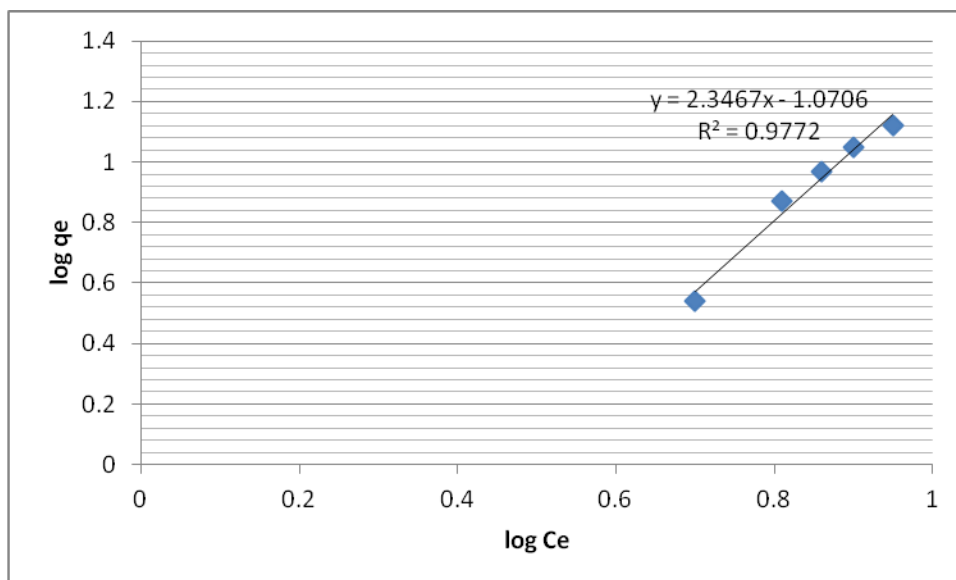


Fig. 8: Freundlich adsorption isotherm for CV dye on RCP.

Fig. 8 shows the Freundlich isotherm model plot for the adsorption CV dye on RCP powder. It is evident from the plot and the values of correlation coefficient ($R^2 = 0.977$) that the experimental data fitted well with the Freundlich isotherm model. Moreover, Freundlich isotherm constant n , (Table 1) was found to be less than 1 indicating that the adsorption of CV by RCP powder is a chemical process [15]. These observations evidence the adequacy of the Freundlich isotherm to describe the adsorption of CV onto RCP and such adsorption mainly occurred on the heterogeneous surface of the RCP powder.

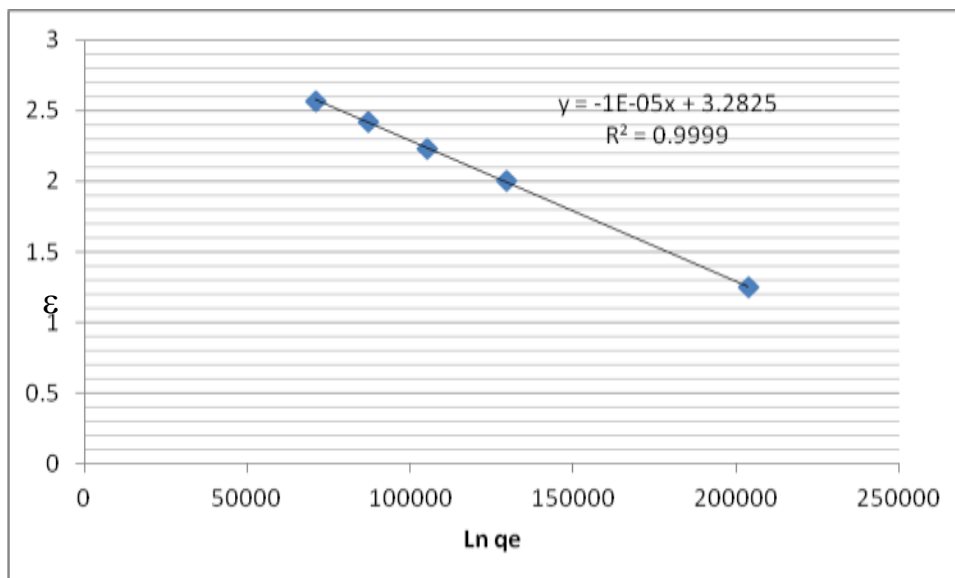


Fig. 9: D–R plot for adsorption of CV onto RCP

The Dubinin – Radushkevich isotherm model for the adsorption of CV onto RCP is depicted in Fig. 9. The D–R isotherm parameters are computed and summarized in Table 1. From the high values of correlation coefficient as shown in Table 1, the D – R isotherm was found to be the best fit for the adsorption of CV by RCP powder. Furthermore, the maximum CV dye sorption capacity of raw cassava peels powder was found to be 26.63 mg/g. The value of E is 0.22KJ/mol.

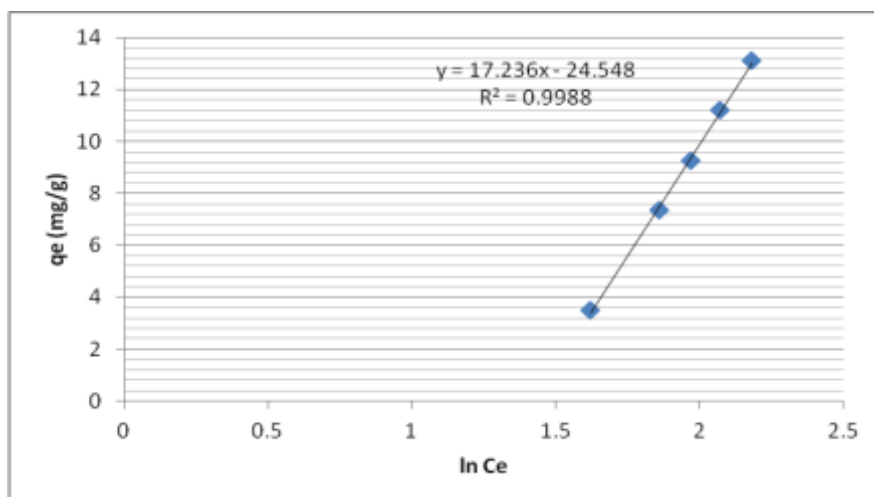


Fig. 10: Temkin isotherm model for CV adsorption onto RCP

The Temkin isotherm model for the adsorption of CV onto RCP is illustrated in Fig. 10 and the Temkin parameters are calculated and summarized in Table 1. It can be observed from Table 1, that the Temkin model was also a good fit for the adsorption of CV onto RCP powder. This reflects the adequacy of Temkin model in explaining the adsorption of CV onto RCP. Furthermore, from Table 1, it can be observed that the values of heat of adsorption, B, was found to be greater than 8kJ/mol, indicating a strong interaction between the CV dye and RCP powder, thus chemical adsorption plays a dominant role in the adsorption process [21]. The Halsey isotherm, the Harkins and Jura isotherm, and the Langmuir isotherm plots (figures not shown) were not found adequate in the description of the adsorption of CV dye onto RCP powder. However, the specific model parameters and correlation coefficient were calculated and included in Table 1.

Table 1: The Isotherm Parameters and Values of Correlation Coefficient for the Adsorption of CV onto RCP powder

Langmuir	q_m (mg/g)	K_L	R^2
	-5.15	-8.52	0.8274
Freundlich	K_F (mg/g)(L/mg) ^{1/n}	n	R^2
	0.085	0.426	0.9772
D-R	q_s (mg/g)	β (mol ² KJ ⁻²)	R^2
	26.63	1.0×10 ⁻⁵	0.9999
Harkins & Jura	A	B	R^2
	3.268	0.925	0.8338
Halsey	K	nH	R^2
	0.034	2.809	0.942
Temkin	B (KJ/mol)	K_T (mol/L)	R^2
	17.23	0.241	0.9988

E

4.8. Adsorption Kinetics

Five kinetic models i.e., pseudo-first-order, pseudo-second-order, power function, Elovich and intraparticle diffusion model as mentioned earlier were applied to investigate the reaction pathways and potential rate determining steps of the adsorption of CV dye onto raw cassava peels powder.

The pseudo-first-order model did not provide a good fit to the experimental data. The first-order rate constant, k_1 , the correlation coefficients, R^2 and the theoretical and experimental equilibrium adsorption capacity q_e are given in Table 2. The plot of $\log(q_e - q_t)$ versus t (not shown) was non linear with low R^2 (0.0685). Moreover, the theoretical and experimental equilibrium adsorption capacity q_e obtained from the plot did not agree (i.e., varied widely), suggesting the inadequacy of the pseudo-first-order model for describing the adsorption kinetics of CV dye onto raw cassava peels powder.

Furthermore, the kinetic data was fitted to the pseudo-second-order model. The pseudo-second-order rate constant, k_2 , the initial adsorption rate, h and the theoretical and experimental equilibrium adsorption capacity are given in Table 2.

The plot of t/q_t against t is depicted in Fig.11. Contrary to the pseudo-first-order model, the fitting of the kinetic data in the pseudo-second-order model showed excellent linearity with high correlation coefficients, R^2 . In addition, there was good agreement between the calculated q_e and the experimental q_e values (i.e., the q_e values were close) indicating that the adsorption of CV by raw cassava peels powder followed the pseudo-second-order kinetics. Hence the adsorption process is controlled by chemisorptions [22]. This suggests that the forming of interaction between the adsorbate and the adsorbent on the external surface of the adsorbent (film diffusion) is the rate limiting step [30].

The power function model and the Elovich model did not provide a good fit to the experimental data (figure not shown). The power function constants, a , b and that of the Elovich model including their correlation coefficients, R^2 are given in Table 3.

The intraparticle diffusion (Weber Morris) model was evaluated to identify the adsorption mechanism. The Weber Morris constant, k_i and C are given in Table 3. The Weber Morris plot for the adsorption of CV onto raw cassava peels powder (figure not shown) was non linear and do not pass through the origin suggesting that intraparticle diffusion was not the rate limiting step. The large intercept indicate the great contribution of surface sorption in the rate limiting step [8, 24].

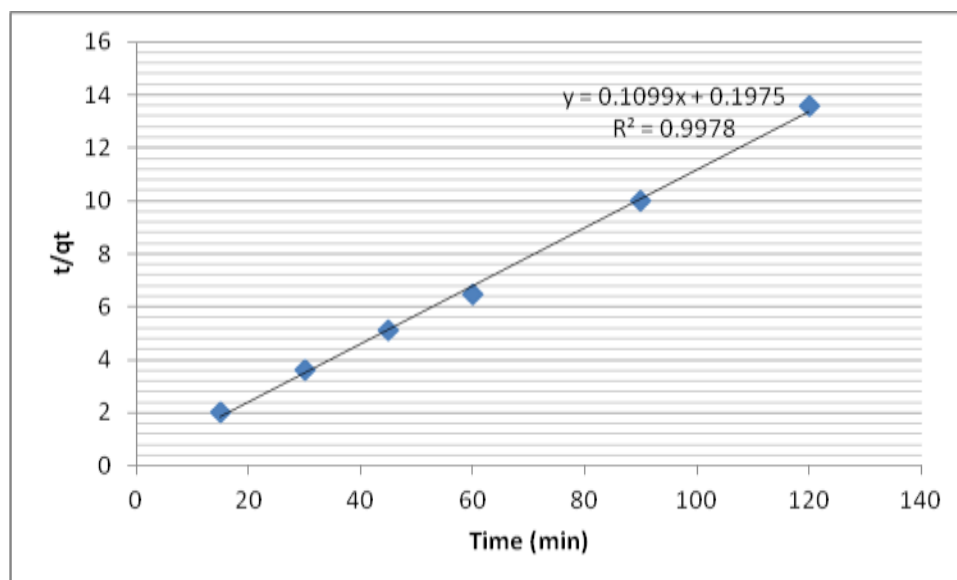


Fig. 11: Pseudo second-order plot for adsorption of CV onto RCP

Table 2: Pseudo-first and second order kinetic model parameters, equilibrium adsorption capacity and values of correlation coefficient for CV dye adsorption onto RCP

Pseudo-First Order Model				Pseudo-Second Order Model			
q_e (exp) (mg/g)	k_1 ($g \cdot mg^{-1} \cdot min^{-1}$)	q_e (cal) (mg/g)	R^2	h ($mg \cdot g^{-1} \cdot min^{-1}$)	K_2 ($g \cdot mg^{-1} \cdot min^{-1}$)	q_e (cal) (mg/g)	R^2
9.31	0.012	0.6859	0.068	5.08	0.060	9.17	0.9978

Table 3: Intra-particle, Elovich, and Power function model parameters with their values of correlation coefficient for CV adsorption onto RCP powder

Intraparticle diffusion			Elovich Model			Power Function		
K_{id}	C	R^2	β	α	R^2	A	B	R^2
mg/g/min	mg/g		$g \cdot min^{-1}$	$mg \cdot g \cdot mg^{-1}$		$g \cdot mg^{-1} \cdot min^{-1}$	$g \cdot mg^{-1} \cdot min^{-1}$	
0.187	7.245	0.542	1.39	2347.25	0.685	6.11	0.087	0.700

4.9. Adsorption Thermodynamics

The linear Van't Hoff equation plot for the adsorption of CV onto RCP powder is shown in Fig.12. Table 4, presents ΔH^0 and ΔS^0 values obtained from the Van't Hoff plot including the calculated ΔG^0 values.

Negative ΔG^0 values obtained at all temperatures (Table 4) indicated the feasibility and the spontaneous nature of CV adsorption onto RCP powder. It was observed that the values of ΔG^0 for the adsorption of CV onto RCP increased with increase in temperature suggesting a rapid and more spontaneous adsorption at higher temperature. The negative ΔH^0 value confirms the exothermic nature of the adsorption process. The negative value of ΔS^0 reveals decreased randomness at the solid/solution interfaces and suggests the adsorption was enthalpy driven [1].

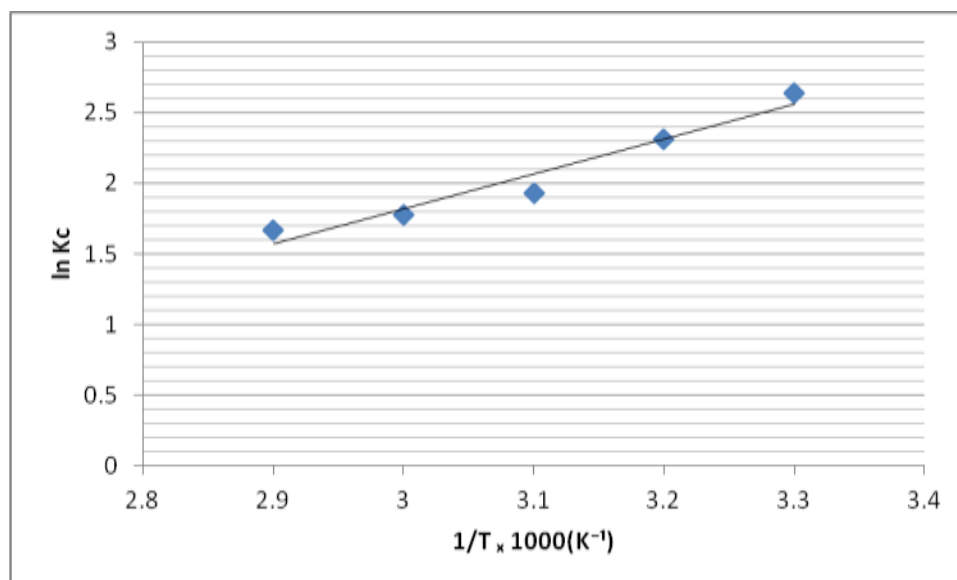


Fig. 12: Van't Hoff plot for the adsorption of CV onto RCP

Table 4: Thermodynamic parameters for the adsorption of CV dye on RCP powder

Temperature (K)	ΔG (KJ/mol)	ΔH (KJ/mol)	ΔS (J/mol. K)
303	-6.65		
313	-6.01		
325	-5.18	-20.536	-46.484
333	-4.93		
343	-4.76		

V. CONCLUSION

The potential of Raw Cassava Peels (RCP) powder as an effective adsorbent for the removal of CV dye from aqueous medium has been identified. The adsorption of CV onto RCP powder was found to be influenced by contact time, adsorbent dose, initial CV concentration, temperature and initial pH of the solution. The optimum adsorption of CV dye was found at pH 10. Temperature had strong influence on the adsorption process and the maximum removal was observed at 303K. The kinetic studies revealed that the adsorption process followed the pseudo-second-order kinetic model. Intraparticle diffusion was not the rate determining step. The study on equilibrium sorption revealed that Dubinin-Radushkevich (D-R) isotherm model gave the best fit to the experimental data. The nature of adsorption of CV on RCP powder was chemical adsorption as inferred from Freundlich isotherm model, Temkin isotherm model and pseudo-second-order kinetic model. The calculated thermodynamic parameters indicated a spontaneous and exothermic nature of the adsorption of CV dye onto RCP powder. The present study showed that RCP powder can be effectively used as an inexpensive and efficient adsorbent without any pretreatment or modification for the treatment of dye effluents and should be utilized by textile and other color related industries for pretreatment of their effluents before disposal to the environment. In addition, activation of the adsorbent could be undertaken to enhance its performance.

REFERENCES

- [1]. S. Chowdhury, and P. Saha, Sea shell powder as new adsorbent to remove basic green4 (malachite green) from aqueous solutions: Equilibrium, kinetic and thermodynamic studies, *Chemical Engineering Journal*, 164, 2010, 168-177.
- [2]. Robinson, T., McMullan, G., Marchant, R., Nigam, P. (2001). Remediation of dyes in textile effluent: a critical review on current treatment technologies with a propose alternative. *J. Biores Tech* 77:247-2752.
- [3]. Hashem, A., Akasha, R. A., Ghith, A., Hussein, D.A. (2007) Adsorbent based on agricultural wastes for heavy metal and dye removal: a review. *Energy Educ. Sci. Technol.* 19:69-86.
- [4]. Chowdhury, S., Mishra, R., Saha, P. (2010) Adsorption thermodynamics, kinetics and isosteric heat of adsorption of malachite green onto chemically modified rice husk. *Dio: 10.1016/ J.Desal.2010.07.047*
- [5]. Allen, S.J. Koumanova B. (2003) Decolourization of water/waste water using adsorption. *J. Univ Chem Technol Metel* 40:175-192.
- [6]. Tahir, S.S., Rauf, N. (2006). Removal of a cationic dye from aqueous solution by adsorption onto bentonite clay. *Chemos.* 63:1842-1848.
- [7]. Bajpai, S. K., Jain, A. (2012) Equilibrium and thermodynamic studies for adsorption of crystal violet onto spent tea leaves. *Water* 4:52-71.
- [8]. Patil, S., Dashmukh, V., Renukdas, S., Patel, N. (2011) Kinetics of adsorption of crystal violet from aqueous solutions using different natural materials. *Inter. J. Env. Sci.* 1(6):1116 – 1134.

- [9]. Hamdaoui, O., Chiha, M. (2007) Removal of Methylene blue from aqueous solution from wheat bran. *Acta. Chim. Slov.* **54**:407-418
- [10]. Malik, R., Rametke, D. S., Wate, S. R. (2006). Adsorption of malachite green on groundnut shell waste based powdered activated carbon. *J. Was. Manag.* **27**:1 – 8.
- [11]. Crini, G. (2006) Non-conventional low-cost adsorbents for dye removal: a review. *J. Bioreso Technol* **97**:1062-1070.
- [12]. Bharathi, K. S., Ramesh, S. T. (2013) Removal of dyes using agricultural waste as low-cost adsorbents: A review. *Appl. Water Sci.* **3**: 773 –790.
- [13]. Al-Ghouti, M. A., Khraishch, M. A. M., Allen, S. J. & Ahmed, M. N. (2003) The removal of dyes from textile wastewater: a study of physical characteristics and adsorption mechanisms of diatomaceous earth. *J. Env. Manag.* **69**: 230 – 237.
- [14]. Ng, C., Losso, J. N., Marshall, W. E., Raw, R. M. (2002) Freundlich adsorption isotherms of agricultural by product based powdered activated carbons in a geosmin-water system. *Bioreso. Techno.*, **85**:131-133.
- [15]. Kumar, P. S., Palaniyappan, M., Priyadharshini, M., Vigensh, A. M., Thonjiappan, A., Sebastina, P. A. F., Tanvir, R. A., Srinath, R. (2013) Adsorption of basic dye onto raw and surface-modified agricultural waste. *Env. Progress and Sustainable Energy*, **33**(1):87 – 98.
- [16]. Kausar, A., Bhatti, H. N., Mackinnon, G. (2013) Equilibrium, kinetics and thermodynamic studies on the removal of U (VI) by low cost agricultural waste. *Colloids & Surfaces B*, **111**:124-133.
- [17]. Singha, B., Das. S.K. (2013) Adsorptive removal of Cu (II) from aqueous solution and industrial effluent using natural agricultural wastes. *Colloids & Surfaces B*, **107**:97-106.
- [18]. Abdelwahab, O. (2007) Kinetic and isotherm studies of copper (II) removal from wastewater using various adsorbents. *Egyptian J. Aqu. Res.* **33**:136.
- [19]. Wang, X. S., Qin, Y. (2005) Equilibrium sorption isotherms for Cu²⁺ on rice bran. *Process. Biochem.*, **40**:677 – 680.
- [20]. Rajoriya, R. K., Prasad, B., Mishra, I. M., Wasewar, K. L. (2007) Adsorption of benzaldehyde on granular activated carbon: kinetics, equilibrium and thermodynamics. *Chem. Biochem. Eng. Q.*, **21**:221 – 224.
- [21]. Pearce, C. I., Lloyd, J. R., Guthrie, J. T. (2003). The removal of colour from textile wastewater using whole bacterial cells: a review. *Dyes and Pigments*, **58**:179-196.
- [22]. Sharma, N., Nnadi, B. K. (2013) Utilization of sugarcane baggase, an agricultural waste to remove malachite green dye from aqueous solution. *J. Mater. Environ. Sci.*, **4**(6):1052-1065.
- [23]. Patil, S., Renukdas, S., Patel, N. (2011). Removal of methylene blue, a basic dye from aqueous solutions by adsorption using teak tree (*Tectona gradnic*) bark powder. *Inter. J. Env. Sci.* **1**(5):711 – 726.
- [24]. Hassanein, T. F. & Koumanova, B. (2010) Evaluation of adsorption potential of the agricultural waste wheat straw on basic yellowish 21. *Journal of the University Chemical Technology and Metallurgy*, **45**(4):407-414.
- [25]. Ho, Y. S. (2003) Removal of copper ions from aqueous solution by free fern. *Water Res.*, **37**:2323-2330.
- [26]. Alshabanat, M., Alsenani, G. & Almufarj, R. (2013) Removal of crystal violet dye from aqueous solutions onto date palm fiber by adsorption technique. *Journal of Chemistry* **2013**: 1-6.
- [27]. Donghee, P., Yeoung-sang, Y. and Jong, M. P. (2010). The fast, present and Future Trends of Biosorption. *Biotechnology and Bioprocessing Engineering*, **15**:86-102.
- [28]. Yaneva Z. L. & Georgieva N. V. (2012) Insights into congo red adsorption on agro-industrial materials: Spectral, equilibrium, kinetic, thermodynamic, dynamic and desorption studies: A review. *International Review of Chemical Engineering (IRECHE)* **4**(2): 127-146.
- [29]. Jyoti, R., Shakti, K. (2013). A comparative study of adsorption behavior of a dye using agro wastes as adsorbents. *J. Env. Sci. Toxicol. And Food Technol.*, **4**(5):91-95.
- [30]. Umpuch, C., Jutarat, B. (2013) Adsorption of organic dyes from aqueous solution by surfactant modified corn straw. *Inter. J. Chem. Eng. Applications*, **4**(3):134 – 139.
- [31]. Wu, C. H. (2007). Adsorption of reactive dyes onto carbon nanotubes: equilibrium, kinetics and thermodynamics. *J. Hazard, Mater.*, **144**:96-98.
- [32]. Iscen, C.F., Krian, I., Iihan, S. (2007) Biosorption of reactive black dyes by *Fenicillium restrictum*: the kinetic study. *J. Hazard Mater.* **143**:335-338.
- [33]. Akar, S. T., Ozcan, A. S., Akar, T., Ozcan, A., Kaynak, Z. (2009) Biosorption of a reactive textile dye from aqueous solutions utilizing an agro-waste. *Desalination* **247**:757-761.
- [34]. Mishra, S., Prakash, D.J., Ramakrishna, G. (2009). *Electronic Journal of Environment, Agricultural and Food Chemistry*, **8**(6):425 – 436
- [35]. Asiagwu, A. K., Owamah, H. I. & Illoh, V. O. (2012) Kinetic and thermodynamic models for the removal of amino-phenol (dye) from aqueous solutions using groundnut (*Arachis hypogea*) shells as the biomass. *Advances in Applied Science Research*, **3**(4):2257-2265.
- [36]. Baek, M.H., Ijagbemi, C.O., Se-Jin, O. and Kim, D.S. (2010) Removal of malachite green from aqueous solution using degreased coffee bean. *J. Hazard. Mater.* **176**:820-828.
- [37]. Hem, L., Garg, V. K., Gupta, R. K. (2007). Removal of a basic dye from aqueous solution by adsorption using parthenium hysterothorus: An Agricultural Waste, *Dyes and Pigment*, **74**:653 – 658.
- [38]. Wang, S., Li, H., Xie, S., Li, S., Xu, L. (2006) Physical and chemical regeneration of zeolitic adsorbents for dye removal in wastewater treatment. *Chemosphere*, **65**: 82 – 87.
- [39]. Crini, G. and Badot, P.M. (2008) Application of chitosan, a natural aminopolysaccharide for dye removal from aqueous solutions by adsorption processes using batch studies: a review of recent literature. *Prog. Polym. Sci.* **33**:399-447.
- [40]. Chandra, T. C., Mirna, M. M., Sudaryanto, Y. and Ismadji, S. (2007). Adsorption of basic dye onto activated carbon prepared from durian shell: Studies of adsorption equilibrium and kinetics. *Chemical Engineering Journal*, **127**(1-3): 121 – 129.

Nnaemeka J. Okoroachal" Adsorptive removal of crystal violet using agricultural waste: Equilibrium, kinetic and thermodynamic studies" *American Journal of Engineering Research (AJER)*, vol. 8, no. 9, 2019, pp. 38-51